

DOI: <https://doi.org/10.37434/tpwj2024.01.01>

INFLUENCE OF COOLING RATE ON MICROSTRUCTURE AND PHASE COMPOSITION OF HAZ OF DUPLEX (DSS) 2205 STEEL IN WET UNDERWATER WELDING

S.Yu. Maksymov¹, G.V. Fadeeva¹, Jia Chuanbao², V.A. Kostin¹,
A.A. Radzievskaya¹, D.V. Vasilyev¹

¹E.O. Paton Electric Welding Institute of the NASU
11 Kazymyr Malevych Str., 03150, Kyiv, Ukraine

²Institute of Materials Joining, Shandong University
17923 Jingshi Road, Jinan 250061, China

ABSTRACT

The article shows the results of the analysis of changes in the microstructure and volumetric particles of phase components of HAZ metal in modeling of welding thermal cycles, inherent in wet underwater welding and welding in air, with the use of the Gleeble-3800 system. The value of cooling rate of different areas of weld metal in wet underwater welding and welding in air was determined. It is shown that as a result of cooling impact of water environment, the cooling rate in wet underwater welding is almost by an order higher than that of welding in air ($w_{13/8} = 8.21$ °C/s — air, in the middle of the weld, and in wet underwater welding it is accordingly $w_{13/8} = 81.70$ °C/s in the middle of the weld, $w_{13/8} = 165.85$ °C/s at the beginning of the weld and $w_{13/8} = 320.51$ °C/s in the weld crater). The change in volumetric particles of phase components of ferrite, austenite and excess phases (chromium Cr₂N nitrides) was determined in the microstructure of HAZ metal depending on the cooling rate. Phase transformations almost completely occur in the high-temperature heat-affected zone (HHAZ) in the temperature range $T = 1300\text{--}800$ °C. Contribution of low-temperature heat-affected zone (LHAZ), temperature range $T = 800\text{--}500$ °C on the change in phase components is negligible. The amount of ferritic and austenitic components and especially the morphology of austenite in the microstructure of HHAZ depend on the cooling rate, as well as the amount of precipitation of excess phases (probably, chromium Cr₂N nitrides)

KEYWORDS: duplex steels, wet underwater welding, input energy, cooling rate, phase composition, austenite, ferrite, microstructure in HAZ, HAZ simulation, thermal welding cycle, Gleeble

INTRODUCTION

The difference in the physical properties of the water environment, first of all, which are 4 times higher than heat capacity and 25 times higher than thermal conductivity compared to air cause a higher cooling rate both in the high-temperature HAZ, which corresponds to the temperature range of 1300–800 °C, and in the low-temperature HAZ, which corresponds to the temperature range of 800–500 °C, relative to other types of welding. Information on the values, that exactly correspond to the cooling rate in wet underwater welding is almost absent in the literature.

ANALYSIS OF EXISTING PROCEDURES FOR DETERMINATION OF INFLUENCE OF THERMAL WELDING CYCLES (TWC) ON HAZ MICROSTRUCTURE.

PROBLEM STATEMENT

To obtain data on the structure and dynamics of phase transformations in duplex stainless steels during welding, it is necessary to investigate the temperature range, which according to the pseudobinary diagram of Fe–Cr–Ni (Figure 1) [1] corresponds to the temperature range of 1200 (1300)–800 °C, depending on

the chemical composition of the steel. There are several methods to obtain data on the temperature-time dependences in the field of phase transformations.

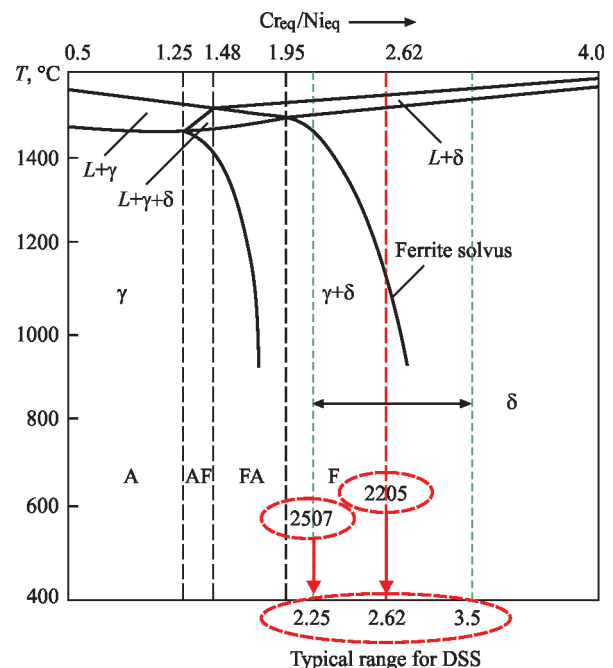


Figure 1. Pseudobinary (Fe–Cr–Ni) diagram, built with the help of the equivalent Cr_{eq}/Ni_{eq} ratio [1]

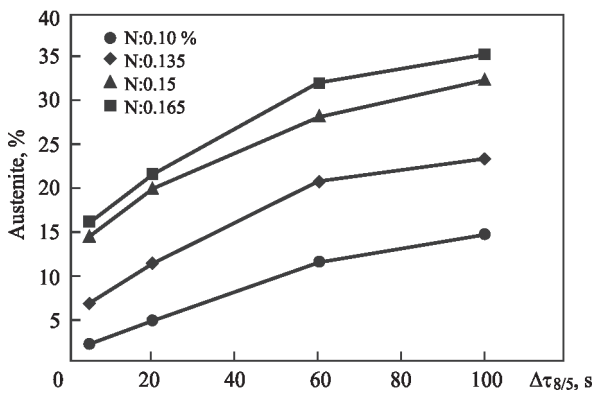


Figure 2. Changes in the content of austenite depending on the time of cooling at different concentrations of nitrogen [6]

One of the methods is a procedure applied to the obtained data on real TWC by recording the temperature and time of the metal being in the temperature range of phase transformations. With the help of thermocouples, the temperature and the time spent in the mentioned temperature range are recorded, to which a certain area of the welded joint is corresponded. Based on these data, the average cooling rate in this range is calculated. The procedure of recording TWC parameters obtained with the help of thermocouples, placed directly in the welding zone or in the HAZ, is very time-consuming and associated with great difficulties, especially when recording TWC in the weld metal. Most often, thermocouples are placed in the HAZ of a welded joint. There are publications where recording of TWC was carried out directly in the weld metal. A new procedure was developed, which uses a combination of thermocouples placed in a pool of a molten weld metal and simultaneously placed on the back side of a weld through drilled holes [2, 3]. This procedure was applied and improved to obtain data on the cooling rates of the weld metal in welding multi-layer joints of superduplex 2507 steel [4].

A new heat treatment method has recently been presented, in which a stationary TIG arc affects a disc-shaped specimen. This method allows covering the en-

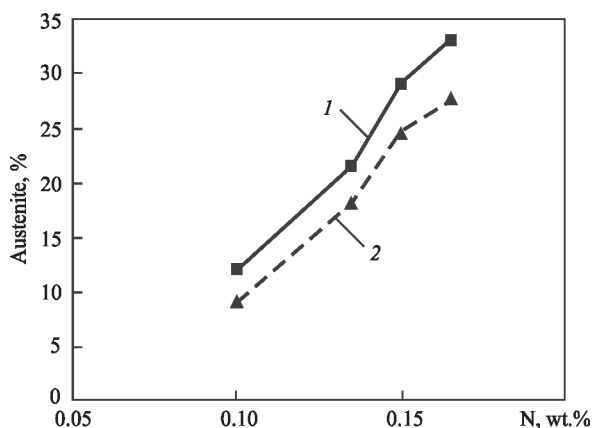


Figure 3. Comparison of austenite content based on the Gleeble simulation (1) and nitrogen content [6] in the HAZ microstructure in real welding [6]

tire temperature range from room to liquidus temperature in a one specimen, thereby significantly reducing a quantity of specimens required to obtain microstructures corresponding to certain temperatures [5].

The procedure of using systems of different modifications of the Gleeble type is well-known, with the help of which, a number of microstructures necessary for research is simulated.

In [6], modeling of microstructures was carried out with the use of the Gleeble system to assess the effect of cooling time and alloying elements on the HAZ microstructure of duplex stainless steel. In addition, submerged arc welding of steel was performed to compare the HAZ microstructures obtained by simulation with Gleeble and in real welding. Modeling of microstructures in the Gleeble-1500 thermomechanical simulator was performed according to the heat treatment mode. The peak temperature $T = 1350$ °C, exposure $\tau = 1$ s, and then the time of cooling from the temperature of 800 to 500 °C ($\Delta\tau_{8/5}$) was 5; 20; 60 and 100 s, respectively.

It was determined that the optimal cooling time ($\Delta\tau_{8/5}$) after welding is from 30 to 60 s for duplex stainless steel with the chemical composition: 0.165 % N–5.5 % Ni–22.3 % Cr–3.2 Mo. It is shown that cooling in the temperature range from 800 to 500 °C in the interval of 30–60 s ensures the content of austenite in the HAZ of not lower than 25 %.

Figure 2 shows changes in the austenite content depending on the cooling time and nitrogen concentration.

Analyzing the given data in Figure 2, it can be noted that the concentration of nitrogen has a greater effect on the austenite content than the cooling time $\Delta\tau_{8/5}$.

Figure 3 shows the content of austenite, which is determined in the microstructure during modeling with Gleeble and in the HAZ microstructure in real welding of steels with a different nitrogen content.

The difference in the amount of austenite in the microstructures simulated by Gleeble and real HAZ obtained during welding is relatively small at the similar cooling time. Thus, the cooling time set by Gleeble can be successfully used as a reference point when choosing welding conditions for duplex steels.

When studying the influence of input energy on the evolution of austenite in the simulated HAZ of duplex 2205 steel, experiments on simulation the welding thermal cycle were carried out in the MMS-200 thermomechanical simulator according to simulated welding thermal cycles corresponding to different input energies [7]. The values of input energy are comparable to those used in submerged arc welding. The morphology of austenite precipitation in the HAZ microstructure depending on the input energy and the

effect of the microstructure on the impact toughness were studied. Thermal cycles were simulated according to the levels of input energy. Input energy was determined with the use of mathematical models by $\tau_{8/5}$, where $\tau_{8/5}$ is the cooling time for the specimen from 800 to 500 °C. Different values of $\tau_{8/5}$: 6; 20; 50; 100; 300 and 600 s were taken to obtain different values of heat input, which corresponded to the next values: 6.2; 11.3; 17.8; 25.2; 43.7 and 61.8 kJ/cm. The calculated levels of input energy correspond to real levels in submerged arc welding from low to superhigh input energy. When determining the share of austenite in the HAZ microstructure, the following conclusion was reached after modeling. The content of austenite lower than 20 % corresponds to the input energy of 0.62 kJ/mm and austenite/ferrite ratio of 1:1 is achieved when the input energy is increased to 6.18 kJ/mm. The value of impact toughness changes and correlates accordingly with the morphology of austenite precipitation in the HAZ.

With the use of the GleebleTM-1500 system, a number of microstructures were simulated, representing those available in the HAZ of welded joints of duplex steels [8]. The simulation took place according to the thermal procedure: heating at a rate of 130 °C/s until reaching the peak temperature $T = 1300$ °C, holding at the peak temperature $\tau = 1$ s and $\tau = 10$ s, then cooling at a rate from 90 to 2.0 °C/s. I.e., the cooling rate from a temperature of 1300 °C was used as a variable. The data obtained as a result of the conducted studies allow assuming that the welding process with low and medium heat inputs, which provide a cooling rate of HAZ in the range from 20 to 50 °C/s, should be the most effective for ensuring the necessary impact toughness of HAZ to -20 °C. This range of cooling rate provides a good balance between the grain size and ferrite/austenite ratio. It was also determined that high cooling rates contribute to both the preservation of ferrite as well as higher deposition of nitrides.

In [9], the study of the cooling time on the microstructure and properties of HAZ in 2507 steel was carried out using the GleebleTM-3800 thermomechanical simulator. The heating rate was 100 °C/s, and the maximum temperature was 1250 °C. The specimens were held for 2 s before cooling. Since the range from 800 to 500 °C was the most uncertain temperature range, and the range from 1200 to 800 °C was a typical range in which the transformation of ferrite into austenite took place, two $\tau_{8/5}$ ranges were chosen — cooling time from 800 to 500 °C and $\tau_{12/8}$ — cooling time from 1200 to 800 °C to study the effect of cooling time on the microstructure and properties of 2507 steel. To analyze and compare the influence of different values of $\tau_{8/5}$ and $\tau_{12/8}$ on HAZ modeling, three groups of cooling parameters were chosen, as given in Table 1.

Table 1. Cooling parameters in temperature ranges

Description of groups	Cooling time in temperature ranges, s	
	$\tau_{8/5}$	$\tau_{12/8}$
1	20; 50; 100; 300	7; 18; 37; 120
2	7; 20; 50; 100	7; 7; 7; 7
3	20; 20; 20	7; 18; 37

As $\tau_{12/8}$ and $\tau_{8/5}$ grew, the content of ferrite decreased and the content of austenite increased, but $\tau_{12/8}$ was a more important cooling parameter that affects the final microstructure of thermal modeling of HAZ of 2507 SDSS. At a ferrite content of about 50 %, $\tau_{8/5}$ was 100 s, whereas $\tau_{12/8}$ was only 37 s. The impact toughness of HAZ grew with an increase in $\tau_{12/8}$; similarly, the resistance to pitting corrosion in the HAZ during welding increased with an increase in $\tau_{12/8}$ and $\tau_{8/5}$, but the effect of $\tau_{12/8}$ was particularly obvious. The most optimal properties were provided when $\tau_{12/8}$ was from 18 to 37 s ($\tau_{8/5} = 20$ s).

In [6], the cooling time in the temperature range from 800 to 500 °C, $\tau_{8/5}$, was chosen as a variable criterion. In [7], $\tau_{8/5}$ was also chosen, then, according to mathematical models, it was converted to the corresponding values of input energy. The rate of cooling from a temperature of 1300 °C was chosen as a variable parameter in [8]. The authors of [9] also studied the cooling time in two temperature ranges, namely $\tau_{12/8}$ and $\tau_{8/5}$.

The results of extensive research on wet underwater welding of duplex steels and the properties of the produced joints are not found in the literature.

As a result of the analysis of studies [6-9] on the application of thermomechanical simulators of the Gleeble type to study the influence of various criteria on the microstructure and phase balance of HAZ of duplex steels, which in turn affect the main technological properties of duplex steels, such as mechanical properties and corrosion resistance, it can be noted, that almost all studies relate to the parameters inherent during welding in air using various technologies. In addition, there was no work that used a real thermal cycle in wet underwater welding of duplex steels to model HAZ.

Therefore, the aim of this examination was to determine and study the effect of cooling rate on the microstructure and phase composition of HAZ of duplex steels, which is simulated by the Gleeble method, using real welding thermal cycles corresponding to wet underwater welding compared to air welding.

RESEARCH METHODOLOGY AND METHODS

The Gleeble-3800 complex was used to study the influence of cooling rate on the microstructure and

Table 2. Chemical composition of 2205 steel (certificate data)

Number according to EN standard	Designation according to EN standard	Steel grade	Content of elements, wt.%								
			C	Mn	P	S	Si	Ni	Cr	Mo	N
1.4462	Kh2CrNiMoN 22-5-3	2205	0.018	1.936	0.03	0.0008	0.303	4.931	22.146	2.557	0.1515

Table 3. Numerical values of TWC parameters

Specimen number	Temperature range, °C; cooling rate w_{cool} , °C/s; cooling time τ , s			
	1300–800		800–500	
	$w_{13/8}$	$\tau_{13/8}$	$w_{8/5}$	$\tau_{8/5}$
1 — air (middle of the weld)	8.21	60.88	5.02	59.78
2 — water (middle of the weld)	81.70	6.12	50.34	5.96
3 — water (beginning of the weld)	165.85	2.94	100.00	3.00
4 — water (crater)	320.51	1.56	161.29	1.86

phase composition of HAZ of duplex 2205 steel under the action of thermal cycle in wet underwater welding compared to welding in air [10]. It was used to model a number of microstructures that correspond to those formed in the HAZ under the influence of welding thermal cycle. The chemical composition of the studied steel is given in Table 2.

To model thermal cycles, which are inherent to those in wet underwater welding and welding in air, the curves were used obtained experimentally applying thermocouples (Figure 4) [11].

Table 3 shows the values of cooling rates and the time spent by the specimens in different temperature ranges during TWC simulation, which correspond to those presented in Figure 4.

Numerical values of parameters were obtained as a result of differentiation of TWC curves.

HAZ simulation was carried out according to the thermal procedure: heating was carried out at a rate of 100 °C/s to a temperature of $T = 1300$ °C, holding time at a peak temperature $\tau = 2$ s, during cooling of the specimens, TWC were simulated, which are

shown in Figure 4 and according to the data presented in Table 3.

To study the effect of cooling rates and cooling time on the microstructure and phase composition of HAZ, two ranges of cooling rates $w_{13/8}$ and $w_{8/5}$ were chosen, which correspond to the high-temperature HHAZ and low-temperature LHAZ. The same applies to the cooling time in the corresponding ranges, $\tau_{13/8}$ and $\tau_{8/5}$. The temperature range of 1200 (1300)–800 °C, depending on the chemical composition of the metal with a typical range, in which the transformation of ferrite into austenite occurs to the greatest extent during cooling. The temperature range of 800–500 °C was chosen to analyze and compare the influence of different ranges on HAZ microstructure during modeling.

If we analyze the values of TWC parameters given in Table 3, namely, the time spent in the temperature range $\tau_{13/8}$, for different areas of the weld in wet underwater welding, i.e.: the middle of the weld is 6.12 s; the beginning of the weld is 2.94 s; weld crater is 1.56 s, so it is less than 10 s. I.e., no value corresponds to the concept, according to which it is recommended to cool a welded joint in the temperature range of 1200–800 °C within 10 s from the time of achieving the optimal microstructure and properties of the welded metal [12].

After thermal modeling, the specimens were cut out in such a way as to cover all areas of the microstructures formed after TWC modeling. The further studies were carried out using optical microscopy (OM) and analytical scanning electron microscopy (SEM). The content of austenite and ferrite in simulated HAZ specimens was determined with the use of the MIPAR image analysis software.

To reveal the microstructure, electrolytic etching was carried out in a 10 % solution of ammonium sulfate at a voltage of 15 V for 20 to 40 s.

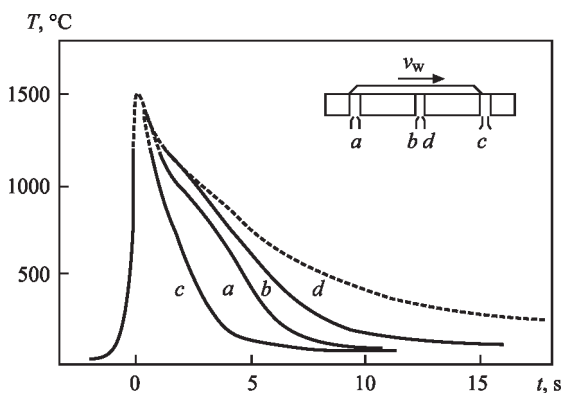


Figure 4. Influence of environment on the nature of welding thermal cycle in different weld areas [11]: *a* — beginning of the weld, specimen No. 3 (water); *b* — middle of the weld, specimen No. 2 (water); *c* — weld crater, specimen No. 4 (water); *d* — middle of the weld, specimen No. 1 (air)

Optical metallography was performed in Ver-samet-2 (USA) and Neophot-32 (Germany) microscopes. Microhardness was measured in M400 Leco device.

RESULTS AND DISCUSSION.

ANALYSIS OF HAZ MICROSTRUCTURES

Figures 5 and 6 show the microstructures in different areas of HAZ simulated at different cooling rates.

When analyzing the microstructures shown in Figures 5 and 6, it should be noted that a change in

the shape of austenite grains is observed, the size of austenite and ferrite grains decreases by an average of 1.5 times, especially in a high-temperature HAZ ($T = 1300\text{--}800\text{ }^{\circ}\text{C}$). The morphology of austenite precipitation also changes. During cooling, grain-boundary austenite (GBA) begins to be formed on the grain boundaries of δ -ferrite, and then acicular (Widmanstaetten) austenite (WA) nucleates along the grain boundaries of δ -ferrite grains and grows in the middle of the grain. In addition to grain-boundary austenite and acicular (Widmanstaetten) austenite, if there is

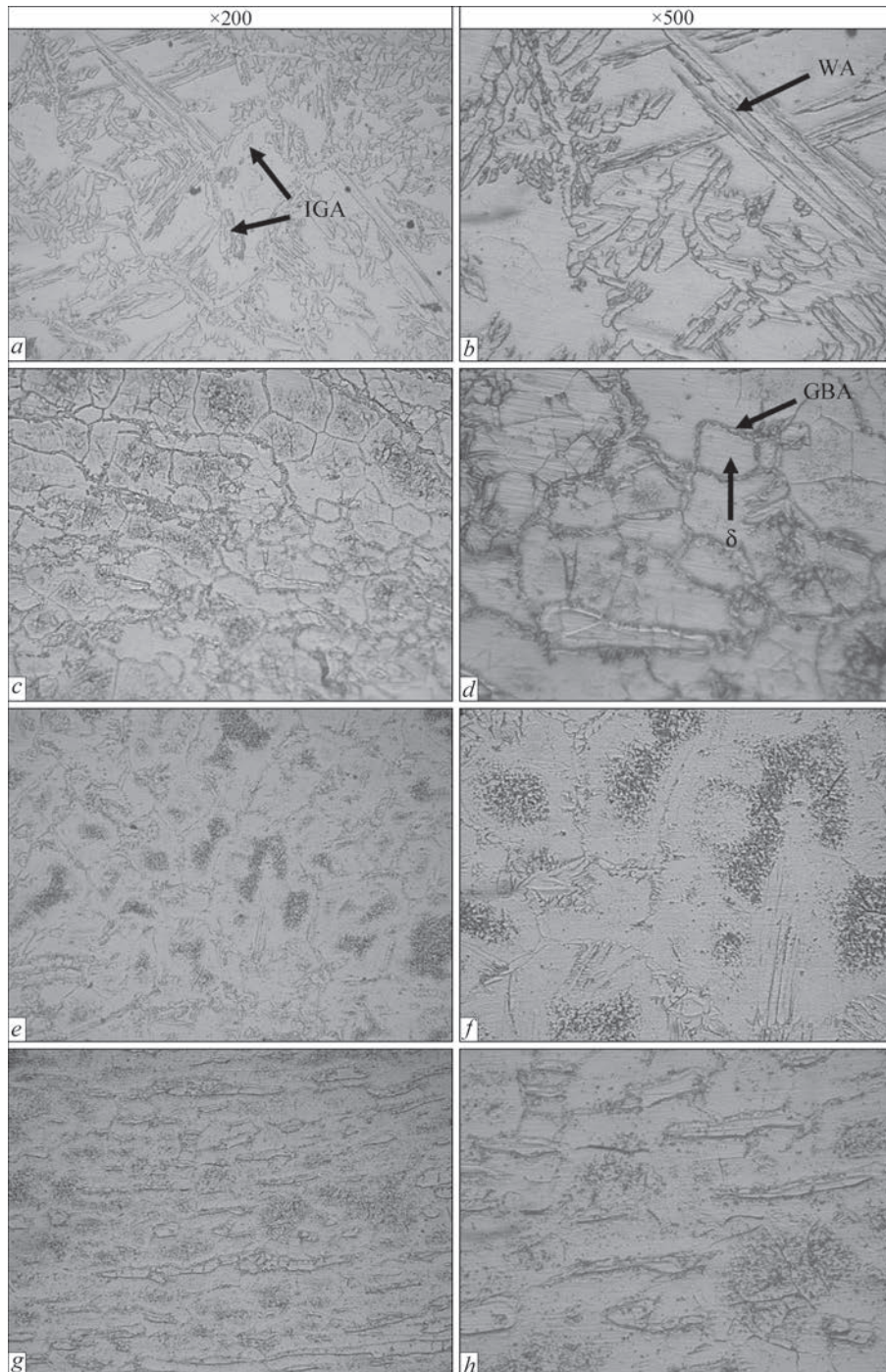


Figure 5. Microstructures of high-temperature HAZ simulated at different cooling rates in the temperature range $T = 1300\text{--}800\text{ }^{\circ}\text{C}$: *a, b* — specimen No. 1, air, $w_{13/8} = 8.21\text{ }^{\circ}\text{C/s}$; *c, d* — specimen No. 2, water — middle of the weld, $w_{13/8} = 81.70\text{ }^{\circ}\text{C/s}$; *e, f* — specimen No. 3, water — the beginning of the weld, $w_{13/8} = 165.85\text{ }^{\circ}\text{C/s}$; *g, h* — specimen No. 4, water — weld crater $w_{13/8} = 320.51\text{ }^{\circ}\text{C/s}$

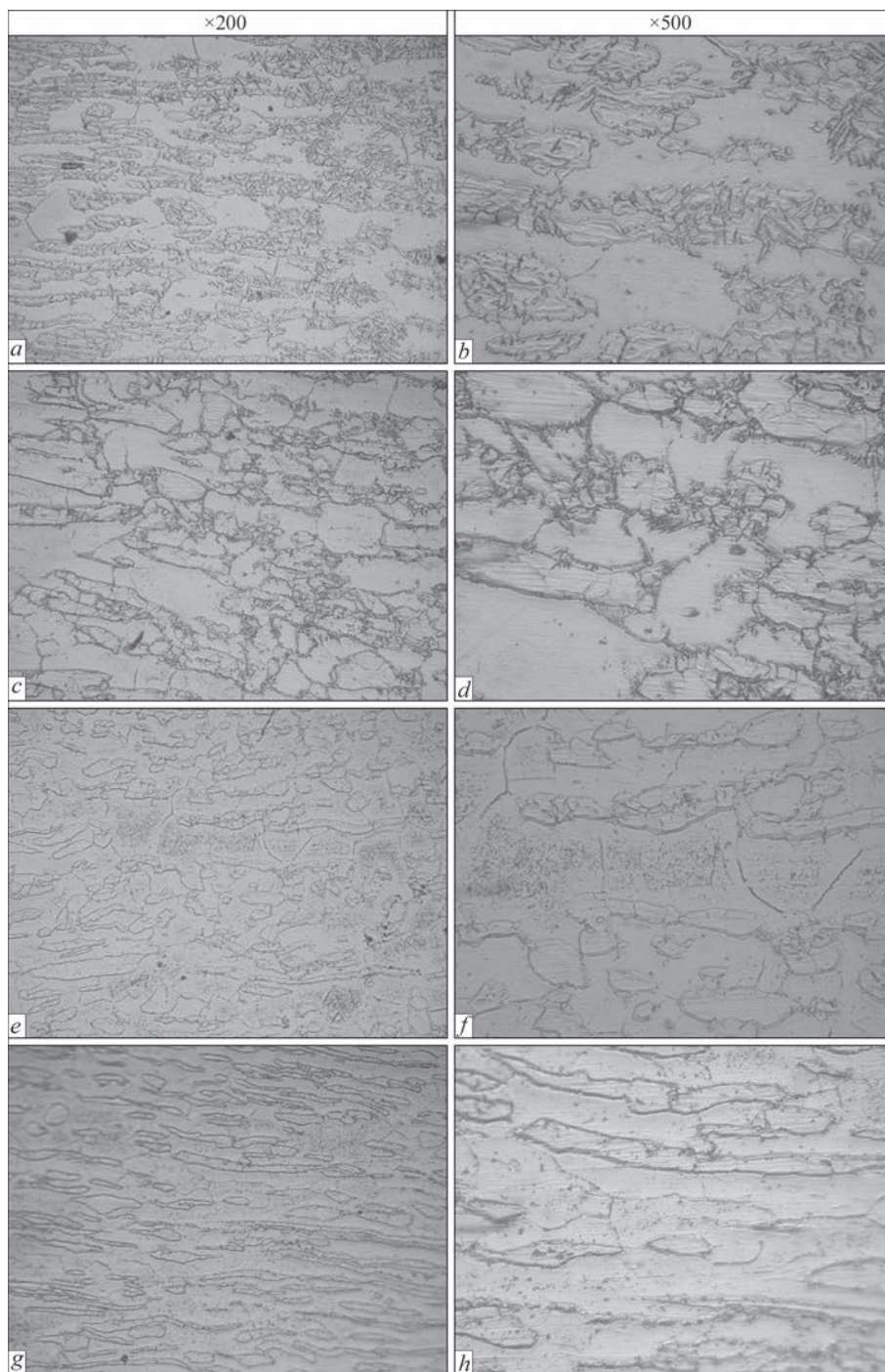


Figure 6. Microstructures of low-temperature HAZ simulated at different cooling rates in the temperature range $T = 800\text{--}500\text{ }^{\circ}\text{C}$: *a, b* — specimen No. 1, air, $w_{8/5} = 5.02\text{ }^{\circ}\text{C/s}$; *c, d* — specimen No. 2, water — middle of the weld, $w_{8/5} = 50.34\text{ }^{\circ}\text{C/s}$; *e, f* — specimen No. 3, water — the beginning of the weld, $w_{8/5} = 100.00\text{ }^{\circ}\text{C/s}$; *g, h* — specimen No. 4, water — weld crater, $w_{8/5} = 161.29\text{ }^{\circ}\text{C/s}$

enough time for diffusion (depending on the cooling rate), intragranular austenite (IGA) may nucleate and grow in the middle of δ -ferrite grains. Since GBA and WA require less supercooling (which is controlled by the cooling rate) for nucleation and growth compared to IGA, they have more time to grow and thus, they dominate in the final microstructure, especially at a low cooling rate.

In general, the microstructure in HAZ of duplex stainless steel changes as follows: during heating, austenite transforms into ferrite, and ferrite

grains grow upon heating to a peak temperature of $T = 1300\text{--}1350\text{ }^{\circ}\text{C}$ (depending on the chemical composition of metal). This temperature corresponds to the single-phase region of ferrite (Figure 1) [1]. During subsequent cooling with a decrease in temperature, ferrite loses its stability and transforms into austenite in the temperature range $T = 1300\text{--}500\text{ }^{\circ}\text{C}$, which corresponds to the two-phase region of austenite and ferrite. The final phase composition of HAZ microstructure is the result after these two processes, namely, heating and then cooling. The final HAZ

Table 4. Size of ferrite grains in the HAZ metal structure depending on the cooling rate

Description of zones	Temperature range, °C	Cooling rate $w_{13/8}$, °C/s			
		8.21	81.70	165.85	320.51
		Grain size $h \times 1$, μm			
I — coarse grain zone	1300–800 HHAZ	100–350×150–450	60–130×100–400	125–250×150–300	80–230×120–300
II — normalization zone	1100–800 HHAZ	50–150×100–160	50–100×100–200	50–155×100–200	50–150×100–200

microstructure mainly depends on the cooling stage, which is characterized by the welding thermal cycle. At a cooling rate $w_{13/8} = 8.21$ °C/s, the presence of all types of austenite is observed, a large amount of grain-boundary austenite, almost along all grain boundaries, as well as intragranular austenite, and acicular (columnar), i.e., Widmanstaetten austenite. The precipitation of excess fine phases was not detected. With an increase in the cooling rate from $w_{13/8} = 8.21$ to $w_{13/8} = 81.70$ °C/s, the morphology of austenite precipitation changes. Precipitation of Widmanstaetten austenite is no longer observed and the amount of intragranular austenite is decreasing. At lower cooling rates, in addition to it, grain-boundary austenite is present, and at a cooling rate $w_{13/8} = 320.51$ °C/s, almost only grain-boundary austenite is present in the microstructure. With an increase in the cooling rate from $w_{13/8} = 81.70$ to $w_{13/8} = 320.51$ °C/s, the precipitation of an excess fine phase is observed, mainly in the coarse ferrite grains, as well as sometimes at the boundaries of austenite and ferrite grains.

When measuring microhardness at a cooling rate $w_{13/8} = 8.21$ °C/s, the most important is austenite in HHAZ, both acicular (Widmanstaetten), as well as grain-boundary austenite, $HV = 3300\text{--}5150$ MPa. A decrease in the microhardness of austenite occurs with an increase in the cooling rate from $w_{13/8} = 8.21$ to $w_{13/8} = 320.51$ °C/s, as in HHAZ ($T = 1300\text{--}800$ °C) as well as in LHAZ ($T = 800\text{--}500$ °C) and is in the range of $HV = 3360\text{--}4390$ MPa. Microhardness of austenite in BM is mainly $HV = 2970\text{--}3090$ MPa, sometimes it reaches $HV = 3300\text{--}3570$ MPa. Such a change in the microhardness of austenite may indicate that the main element that affects the microhardness of austenite is nitrogen. Microhardness of austenite depends on its content in the lattice. Microhardness of ferrite at all cooling rates is from $w_{13/8} = 8.21$ °C/s to $w_{13/8} = 320.51$ °C/s, both in HHAZ ($T = 1300\text{--}800$ °C) as well as in LHAZ ($T = 800\text{--}500$ °C) is almost the same and equals to $HV = 2300\text{--}2900$ MPa. Microhardness of ferrite in the base metal is almost the same $HV = 2300\text{--}2570$ MPa, sometimes it reaches $HV = 2970$ MPa, i.e., microhardness of ferrite remains unchanged both in HAZ as well as in the base metal.

Table 4 shows the size of ferrite grains in the simulated HAZ.

At all cooling rates, the refinement of ferrite grains in the II temperature zone compared to the I zone is observed. At a cooling rate $w_{13/8} = 320.51$ °C/s, the size of ferrite grains in HHAZ is the lowest and is equal to $80\text{--}230 \times 120\text{--}300$ μm (I zone), and $50\text{--}150 \times 100\text{--}200$ μm (II zone) (Table 4).

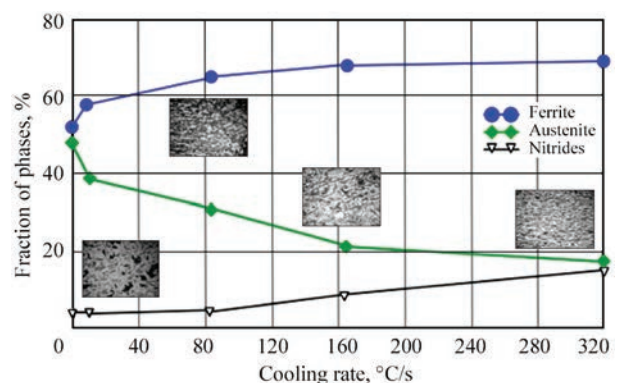
This data reaffirms that the time spent in the temperature range of phase transformations is not the only factor that affects the completeness of phase transformations, as well as depends on the size of ferrite grains, i.e., on the diffusion of both ferrite- as well as austenite-forming elements: nitrogen, nickel, manganese, and primarily on the nitrogen diffusion coefficient, since it is higher than other elements: nickel, manganese, chromium and molybdenum.

PHASE COMPOSITION OF HAZ

Figure 7 shows changes in volumetric particles of phase components, ferrite, austenite and excess phase (probably, precipitation of Cr_2N chromium nitrides) depending on the cooling rate in the simulated HAZ of duplex steel in the temperature range $T = 1300\text{--}800$ °C determined with the use of the MIPAR software for image analysis.

Figure 8 shows microstructures of the simulated HAZ at different cooling rates corresponding to the temperature range $T = 1300\text{--}800$ °C, which were used to determine the phase composition by means of the MIPAR software.

Table 5 shows the values of volumetric particles of phase components of the simulated HAZ at different cooling rates in the temperature range


Figure 7. Phase composition of HAZ of duplex steel depending on the cooling rate in the temperature range of 1200 (1300)–800 °C

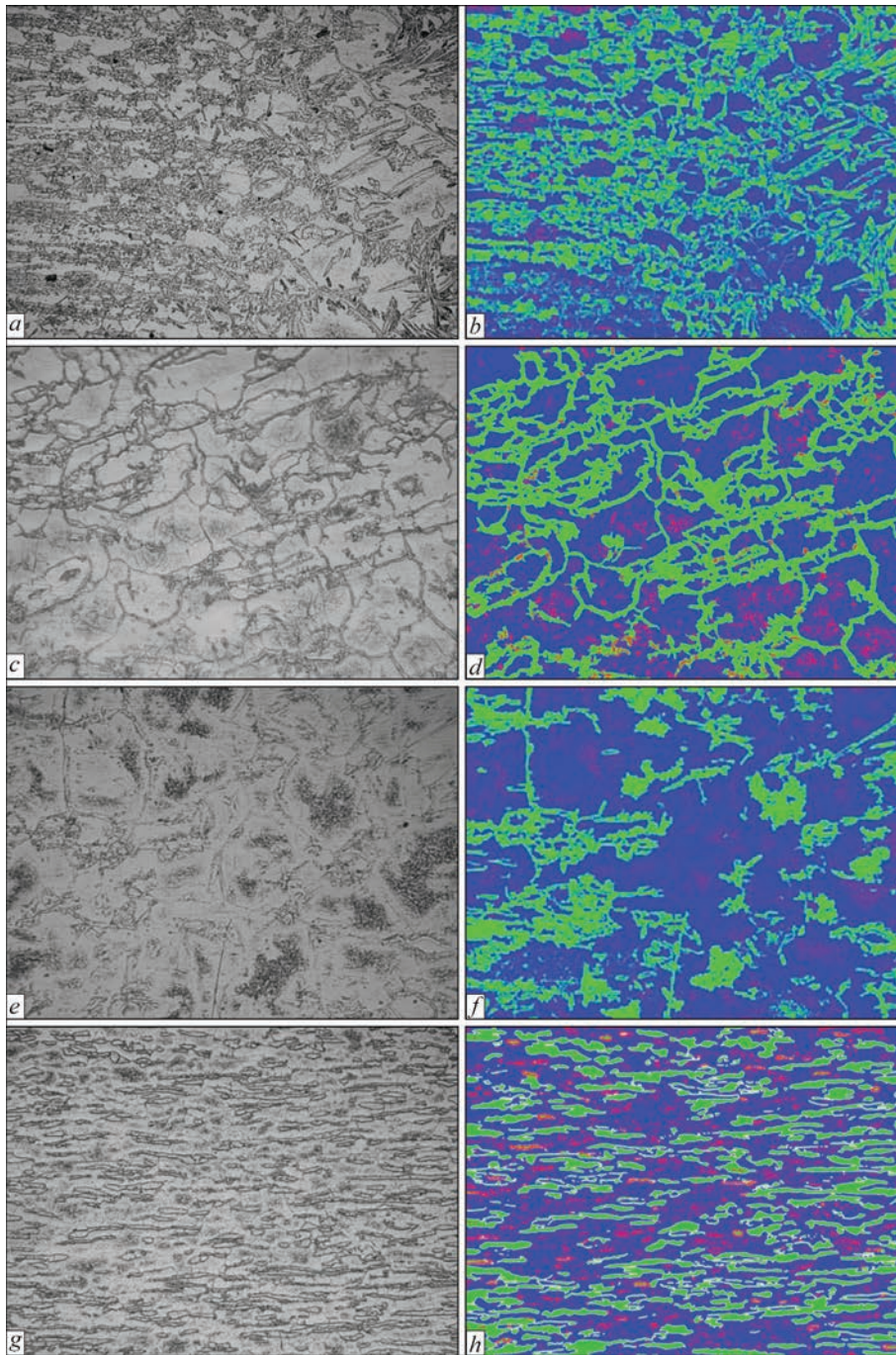


Figure 8. Microstructures ($\times 100$) of simulated HAZ at different cooling rates, processed with the use of the MIPAR software: *a, b* — specimen No. 1, air, $w_{13/8} = 8.21$ °C/s; *c, d* — specimen No. 2, water — middle of the weld, $w_{13/8} = 81.70$ °C/s; *e, f* — specimen No. 3, water — beginning of the weld, $w_{13/8} = 165.85$ °C/s; *g, h* — specimen No. 4, water — weld crater. $w_{13/8} = 320.51$ °C/s. Matrix — ferrite; grain — austenite; small inclusions — nitrides

Table 5. Phase composition of HAZ simulated at different cooling rates in the temperature range $T = 1300\text{--}800$ °C

HAZ cooling rate, °C/s	Fraction of phases, %		
	δ , ferrite	γ , austenite	Excess phase (fine)
Base metal	52.000	48.000	—
8.21	57.499	38.674	3.236
81.70	64.644	30.268	3.746
165.85	67.696	20.965	8.606
320.51	68.848	17.733	13.437

$T = 1300\text{--}800$ °C, which were determined with the use of the MIPAR software.

If we compare the phase composition of the microstructures at different cooling rates in the high-temperature range of HHAZ ($T = 1300\text{--}800$ °C), then with an increase in the cooling rate from $w_{13/8} = 8.21$ to 320.51 °C/s, the content of austenite decreases more than twice, and the content of ferrite, on the contrary, increases by 1.2 times.

The data given in Table 5, indicate that the transformation of ferrite into austenite occurs almost com-

pletely in HHAZ in I and II zones in the temperature range $T = 1300\text{--}800\text{ }^{\circ}\text{C}$, and the completeness of the transformation depends on the time spent in this range and on the size of ferrite grains. At the same time, the morphology of austenite precipitation depends to a greater extent on the time spent in this temperature range. At a cooling rate $w_{13/8} = 8.21\text{ }^{\circ}\text{C/s}$, the time spent in the temperature range $T = 1300\text{--}800\text{ }^{\circ}\text{C}$ is 60.88 s, in the microstructure the presence of all types of austenite is observed: grain-boundary, Widmanstaetten and intragranular. Precipitation of excess phases is not observed. When the cooling rate grows to $w_{13/8} = 320.51\text{ }^{\circ}\text{C/s}$, the morphology of austenite precipitation changes, precipitation of acicular (Widmanstaetten) austenite is not observed anymore and the amount of intragranular austenite decreases. At all cooling rates, grain-boundary austenite is present, and at a cooling rate $w_{13/8} = 320.51\text{ }^{\circ}\text{C/s}$, in the microstructure, mostly only grain-boundary austenite is present. With an increase in the cooling rate from $w_{13/8} = 81.70$ to $320.51\text{ }^{\circ}\text{C/s}$, precipitation of tiny excess phases is observed mainly in the coarse ferrite grains, as well as sometimes at the boundaries of austenite and ferrite grains.

The analysis of chemical elements in the high-temperature HAZ ($T = 1300\text{--}800\text{ }^{\circ}\text{C}$) revealed precipitation of excess phases with an increased content of chromium in both austenite and ferrite. This is explained by the fact that at a high cooling rate, the transformation of ferrite into austenite does not occur to the full extent, the amount of austenite precipitation decreases, and an excess phase with a higher chromium content is observed in ferrite grains (probably, Cr_2N). At a cooling rate $w_{13/8} = 320.51\text{ }^{\circ}\text{C/s}$ in the I zone ($T = 1300\text{--}800\text{ }^{\circ}\text{C}$), in ferrite grains, with the use of a scanning microscope (SEM), rod-type inclusions of up to $10\text{ }\mu\text{m}$ in length with a chromium content of 23.2–24.14 % were revealed. Chromium Cr_2N nitrides found in [13] also have a rod-like appearance. This indicates that these are probably Cr_2N chromium nitrides, since the base metal contains 0.1515 % of nitrogen and the carbon content is lower than 0.02 % (0.018 %). Since the process of transformation of ferrite into austenite is a diffusion process, the completeness of the transformation of ferrite into austenite, that is, the final phase composition of HAZ microstructure, depends on the diffusion coefficients of ferrite-forming elements and austenite-forming elements, primarily nitrogen (Table 5, Figure 7).

The obtained data may indicate that the completeness of phase transformations depends not only on the cooling rate and time spent in the temperature range, where the transformation of ferrite into austenite occurs, but also on the size of ferrite grains.

CONCLUSIONS

1. The influence of cooling rate on the microstructure and phase composition in the simulated HAZ of duplex 2205 steel with the use of Gleeble-3800 was studied. Simulated microstructures with cooling rates from $w_{13/8} = 8.21$ to $320.51\text{ }^{\circ}\text{C/s}$, as well as from $w_{8/5} = 5.02$ to $161.29\text{ }^{\circ}\text{C/s}$ showed a change in the phase composition of austenite and ferrite. To the greatest extent, the change in the volumetric particles of phases occurs at the cooling rates $w_{13/8}$ — from 81.70 to $320.51\text{ }^{\circ}\text{C/s}$, which correspond to the cooling rates in wet underwater welding in the high-temperature HAZ.

2. When the cooling rate $w_{13/8}$ grows from 8.21 to $320.51\text{ }^{\circ}\text{C/s}$, the volumetric fraction of austenite decreases by 2.18 times (from 38.67 to 17.73 %), the volumetric fraction of ferrite, on the contrary, grows by 1.2 times (from 57.41 to 68.85 %).

3. The content of austenite at the cooling rates from $w_{13/8} = 81.70$ to — $320.51\text{ }^{\circ}\text{C/s}$, which correspond to the cooling rates in wet underwater welding, decreases from 30.27 to 17.73 %. The main part is formed by grain-boundary and intragranular austenite. At the cooling rates $w_{13/8} = 8.21$ and $5.02\text{ }^{\circ}\text{C/s}$, which are inherent during welding in air, all types of austenite are observed: grain-boundary, acicular (Widmanstaetten), and intragranular austenite.

4. The phase transformation of ferrite into austenite occurs mostly in the high-temperature HAZ, in the temperature range $T = 1300\text{--}800\text{ }^{\circ}\text{C}$.

5. The completeness of phase transformation of ferrite into austenite depends on the cooling rate, i.e., the time spent in a given temperature range, and also on the sizes of ferrite grains.

6. The amount of excess phase precipitation (probably, chromium Cr_2N nitrides) is directly proportional to the cooling rate and also depends on the amount of the austenitic component. With an increase in the cooling rate, the amount of chromium nitride precipitation almost four times increases, i.e. from 3.24 to 13.44 %.

7. With an increase in the cooling rate, a decrease in the size of ferrite grains is observed.

8. The amount of ferritic component grows with an increase in the cooling rate, but it is not critical and amounts to 68.85 %, i.e., it does not reach 70 %, which is allowed by recommendations and standards. Despite the fact that the cooling rate in wet underwater welding is by an order higher than during welding in air, due to the refinement of the microstructure, a critical increase in the fraction of ferrite is not observed.

9. The obtained data can be used when choosing the modes and a type of weld metal alloying in wet underwater welding.

10. Recommendations for the range of welding input energy values $Q = 0.5\text{--}2.5$ kJ/mm for 2205 steel developed for welding in air and which contribute to obtaining a balanced phase composition of HAZ of duplex stainless 2205 steel, should be subjected to correction in wet underwater welding.

11. The results of studies on the influence of cooling rate on the microstructure and phase composition of HAZ of duplex (DSS 2205) steel simulated by the Gleeble-3800 method correspond only to those TWC and those chemical compositions of the base metal that are used in this study.

REFERENCES

1. Verma, I., Taiwade, R., R.V. (2017) Effect of welding processes and conditions on the microstructure, mechanical properties and corrosion resistance of duplex stainless steel weldments — A review. *J. of Manufacturing Processes*, **25**, 134–152.
2. Bermejo, V.M.A., Hurtig, K., Hosseini, V.A. et al. (2016) Monitoring thermal cycles in multi-pass welding. In: *Proc. of the 7th Int. Swedish Production Sym. — SPS-16, (Lund, Sweden, 25–27 October)*.
3. Bermejo, V.M.A., Hurtig, K., Karlsson, L., Svensson, L.E. (2017) A step forward in understanding superduplex multi-pass welds by monitoring thermal cycles. In: *Proc. of the 70th IIW Annual Assembly (Shanghai, China, 28 June 2017)*.
4. Bermejo, M.A.V., Daniel, E., Hurtig, K., Karlsson, L. (2019) *A new approach to the study of multi-pass welds microstructure and properties of welded 20-mm-thick superduplex stainless steel*. <http://www.researchgate.net/publication/331715232>
5. Hosseini, V.A., Karlsson, L., Engelberg, D., Wessman, S. (2018) Time-temperature — precipitation and property diagrams for super duplex stainless steel weld metals. *Weld. World*, **62**, 517–533.
6. Hsienh, R.-J., Liou, H.-Y., Pan, Y.-Ts. (2001) Effects of cooling time and alloying elements on the microstructure of the Gleeble-simulated heat-affected zone of 22 % Cr duplex stainless steels. *J. of Mater. Eng. and Performance*, **10**(5), 526–536.
7. Wu, T.-h., Wang, J.-j., Li, H.-b et al. (2018) *Effect of heat input on austenite microstructural evolution of simulated heat affected zone in 2205 duplex stainless steel*. DOI: <https://doi.org/10.1007/s42243-018-0134-z>
8. Lippold, J.C., Varol, I., Baeslack, W.A. (1994) The influence of composition and microstructure on the HAZ toughness of duplex stainless steels at -20 °C. *Welding J., Res. Suppl.* **1**, 75–79.
9. Zhou, Y., Zou, D., Li, K. et al. (2018) Effect of cooling time on microstructure and properties of 2507 super duplex stainless steel welding heat-affected zone. *Mat. Sci. Forum*, **940**, 5358.
10. Grigorenko, G.M., Kostin, V.A., Orlovsky, V.Yu. (2008) Current capabilities of simulation of austenite transformations in low-alloyed steel welds. *The Paton Welding J.*, **3**, 22–24.
11. Hasui, A., Suga, Y. (1980) On cooling of Underwater Welds. *Transact. of the JWS*, **11**(1). April.
12. Geipl, H. (1989) MAGM-Schweissen von Rorrosions beständig Duplex-Stählen 22Cr5(9)Ni3Mo. Entfluss von schutzgas- und werfahrenvarianten. *Linde – Sonderdruck*, **146**, Hällriegels – kreuth.
13. Hu, Y., Shi, Y., Shen, X., Wang, Zh. (2017) Microstructure, pitting corrosion resistance and impact toughness of duplex stainless steel underwater dry hyperbaric flux-cored arc welds. *Materials*, **10**, 1443, www.mdpi.com/journal/materials

ORCID

S.Yu. Maksymov: 0000-0002-5788-0753

CONFLICT OF INTEREST

The Authors declare no conflict of interest

CORRESPONDING AUTHOR

S.Yu. Maksymov

E.O. Paton Electric Welding Institute of the NASU

11 Kazymyr Malevych Str., 03150, Kyiv, Ukraine.

E-mail: maksimov@paton.kiev.ua

SUGGESTED CITATION

S.Yu. Maksymov, G.V. Fadeeva, Jia Chuanbao, V.A. Kostin, A.A. Radzievskaya, D.V. Vasilyev (2024) Influence of cooling rate on microstructure and phase composition of HAZ of duplex (DSS) 2205 steel in wet underwater welding. *The Paton Welding J.*, **1**, 3–12.

JOURNAL HOME PAGE

<https://patonpublishinghouse.com/eng/journals/tpwj>

Received: 06.09.2023

Received in revised form: 13.10.2023

Accepted: 16.01.2024

